

## NOVEL ENERGY HARVESTING ANTENNA DESIGN USING A PARASITIC RADIATOR

Jung-Ick Moon<sup>1</sup> and Young-Bae Jung<sup>2, \*</sup>

<sup>1</sup>Radio Technology Research Department, Electronics and Telecommunications Research Institute, 138 Gajeong-no, Yuseong-gu, Daejeon, Republic of Korea

<sup>2</sup>Department of Electronics and Control Engineering, Hanbat National University, 16-1 Duckmyong-dong, Yuseong-gu, Daejeon, Republic of Korea

**Abstract**—A novel energy harvesting antenna for various wireless transceivers is proposed. This antenna is composed of two parts, the main and the parasitic radiator. The main radiator has the same role as a general element antenna, i.e., to transmit and receive the RF signal. The parasitic radiator is used to gather the RF power from the main radiators, which mostly do not contribute the main radiator's electrical performance. Thus, we can generate DC power using the dissipated RF energy that is radiated from the main radiator. The main radiator is designed as a printed dipole and the parasitic radiator has a two-turn loop structure fabricated on a substrate. The main radiator is vertically placed on the ground and inserted in the rectangular slit of the substrate of the parasitic radiator. The height of the parasitic radiator can be controlled by two supporters. In the design process, we analyzed how the antenna performance changed when adjusting the height of the parasitic radiator and thus determined its optimal height.

### 1. INTRODUCTION

Energy harvesting is the process of accumulating and storing ambient energy from various sources in the surrounding environment in energy storage components. These energy sources may include electrostatic, kinetic, piezoelectric, biomechanical, photoelectric, thermoelectric, and ambient-radiation sources.

---

*Received 18 August 2013, Accepted 11 September 2013, Scheduled 17 September 2013*

\* Corresponding author: Young-Bae Jung (ybjung@hanbat.ac.kr).

In recent years, the use of wireless devices is growing in many applications, such as mobile phones and sensor networks. RF energy is currently broadcasted from billions of radio transmitters around the world, including mobile telephones, handheld radios, mobile base stations, and television/radio broadcast stations. The ability to harvest RF energy, from ambient or dedicated sources enables the wireless charging of low-power devices and has other benefits associated with product design, usability, and reliability. Battery-based systems can be trickle-charged to eliminate battery replacement requirements or to extend the operating lifetimes of the systems using disposable batteries. Battery-free devices can be designed to operate upon demand or when sufficient charge is accumulated [1, 2]. In this area, most of the research has focused on how to obtain as much energy as possible from RF energy resources such as base stations and Wi-Fi routers via air-space, and solutions have been proposed mainly for multi-band and wideband receivers and highly efficient RF-DC conversion circuits [3–11]. And some researches have been focused on the efficient technique for maximum power point tracking (MPPT) of an energy harvesting device. It is based on controlling the device voltage at the point of maximum power [12, 13].

However, while many researchers have made an effort to increase the receiving RF power, the RF energy accumulated from air-space is very limited, at less than  $1 \mu\text{W}$ . Mikeka et al. conducted several experiments using highly efficient receivers that were capable of receiving digital TV signals in the range of  $-40 \sim -20 \text{ dBm}$  in Tokyo. However, there are no devices except a digital thermometer that could be operated using the DC power converted from the received RF power [9–11].

In this paper, we propose a novel antenna structure for RF energy harvesting. As mentioned above, it is difficult to obtain enough energy from free space to power electronic devices. Therefore, we attempted to gather energy using a parasitic radiator directly from the main antennas of base stations and repeaters, which radiate RF signals. Using this concept, we were able to obtain much more energy than conventional energy harvesting receivers. In addition, the transmitters maintain nearly their original level of performance, especially in terms of the antenna gain and radiation pattern, as the proposed antenna mainly receives the dissipated power which does not contribute to the performance of the radiator.

## 2. PROPOSED ANTENNA DESIGN

### 2.1. Antenna Structure

The proposed energy harvesting antenna structure is depicted in Figure 1. As shown in Figure 1(a), the proposed antenna is mainly composed of two individual radiators, the main radiator and the parasitic radiator. The main radiator has the role of signal transmission for the communications service and thus can be thought of as the main antenna of a base station or repeater. The parasitic radiator couples the RF power, which mostly does not contribute to the main performance of the main radiator, as the harvested signal is radiated out of a 3-dB beam width of the main radiator. Thus, the main radiator can maintain its original level of performance with only a limited amount of deviation.

There are many types of radiators used for wireless communications. We choose the printed dipole radiator, which is widely used for base station antennas due to the merit of wideband and high gain characteristics as well as easy fabrication. The parasitic radiator has a loop structure. The loop antenna can be designed in various shapes, such as a circle, a square, a rectangle, a triangle and others. In particular, a resonant loop has a circumference approximately equal to one

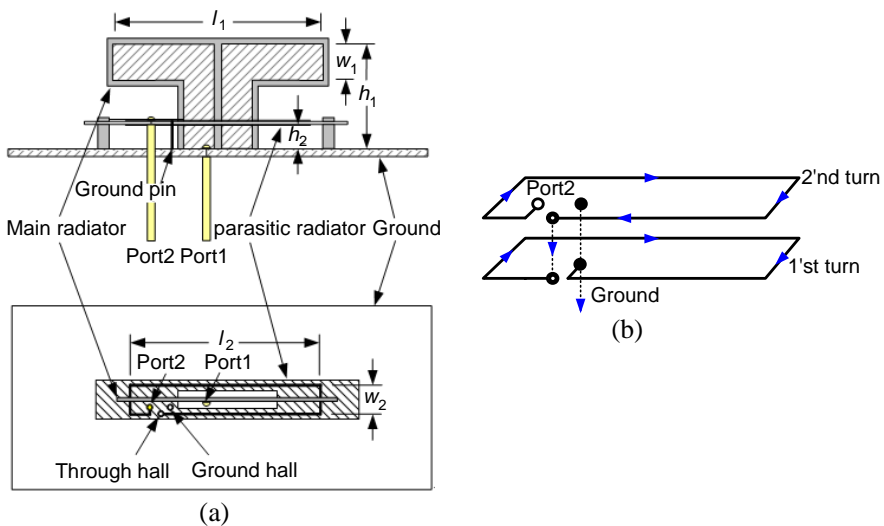


**Figure 1.** Proposed energy harvesting antenna structure. (a) Side-view and top-view. (b) Two-turn loop structure of parasitic radiator.

wavelength (while also being resonant at odd multiples of the wavelength). Compared to the dipole or folded dipole, it transmits less toward the sky or ground, giving it a somewhat higher gain (about 10% higher) in the horizontal direction. The loop can output a RMS (Root Mean Square) voltage  $E$  from a RMS magnetic field strength  $B$  at a given angle between the magnetic field lines and the loop frame normal direction [14].

$$E = 2 \cdot N \cdot A \cdot f \cdot B \cdot \cos \theta$$

Here,

$N$ : the number of turns.

$A$ : area of each winding [ $\text{m}^2$ ].

$f$ : operating frequency [GHz].

$B$ : RMS value of the magnetic induction [Tesla].

Thus, the loop antenna is very suitable for receive RF power in all directions from the main radiator. In this design, the printed rectangular loop element encloses the main radiator, the printed dipole, which is inserted in the rectangular slit of the parasitic radiator's substrate, as shown in the lower diagram of Figure 1(a). Figure 1(b) shows the two-turn loop structure of the parasitic radiator in detail as designed with a dielectric substrate, which is not shown in the figure to clarify the loop structure. The multi-turn loop provides a high quality factor, known as the  $Q$ -factor, compared to a single turn. Therefore, it has a higher gain characteristic in a narrow frequency bandwidth. Figure 2 shows the phenomena of RF signal radiation from an ideal half dipole over the ground. The vertical radiation pattern determines the wave angle of the antenna; the wave angle is the angle at which the radiation is maximized. In the vertical plane perpendicular to the ground, the dipole radiates equal energy in all directions. Using ray analysis, A and A' radiate in opposite directions, and A'' is the reflected signal of A' by the ground in the same direction as A. B'', the reflected ray of B', is reflected in the same direction as B. In this situation, the important issue is the phase difference between A and A'' and between B and B''. The phase difference is created by the path-length difference plus any phase shift at the reflection point itself. Horizontally polarized rays undergo a  $180^\circ$  phase shift when reflected from perfect ground. The eventual phase relationship between the direct and the reflected horizontally polarized wave will depend primarily on the height of the dipole over the reflection ground. If at a very distant point the rays at points A and A'' are in-phase, then their combined field strength will be at a maximum and will be equal to the sum of the magnitudes of the two rays. If they are out-of-phase, the resulting field strength

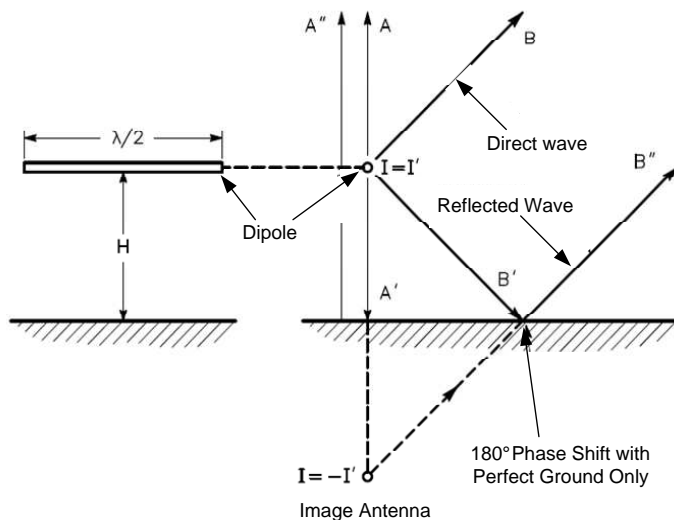


**Figure 2.** RF energy radiation from a ideal half dipole by the electrical ground mirror.

will be less than the sum of the individual rays. If  $A$  and  $A''$  are identical in magnitude and are 180 out-of-phase, total cancellation will occur [15]. The parasitic radiator of the proposed antenna is used mainly to receive the RF power radiated at some angle from the main radiator, which does not contribute to the electrical performance of the main radiator, as explained above. Thus, we can obtain much RF energy from the main radiator of wireless transmitters (or transceivers) without degrading the performance of the main radiator.

## 2.2. Design Parameter of the Proposed Antenna

Using the proposed antenna structure, we designed the energy harvesting antenna to be operated in the frequency band of WCDMA (Wideband Code Division Multiple Access) service, 2.13~2.15 GHz, in the Republic of Korea. The WCDMA service is the one of the most popular services with LTE (Long Term Evolution) in Korea.

The main radiator is designed with a RF-35 substrate of Taconic Inc. ( $\epsilon_r = 3.5$ ,  $\tan \delta = 0.0018$ ,  $t = 0.78$  mm). The width ( $w_1$ ) and the length ( $l_1$ ) of the main radiator are 16 mm and 68 mm, respectively. Its height is 39 mm. The parasitic radiator is designed with FR4 substrate ( $\epsilon_r = 4.3$ ,  $\tan \delta = 0.02$ ,  $t = 1$  mm). The width ( $w_2$ ) of the rectangular

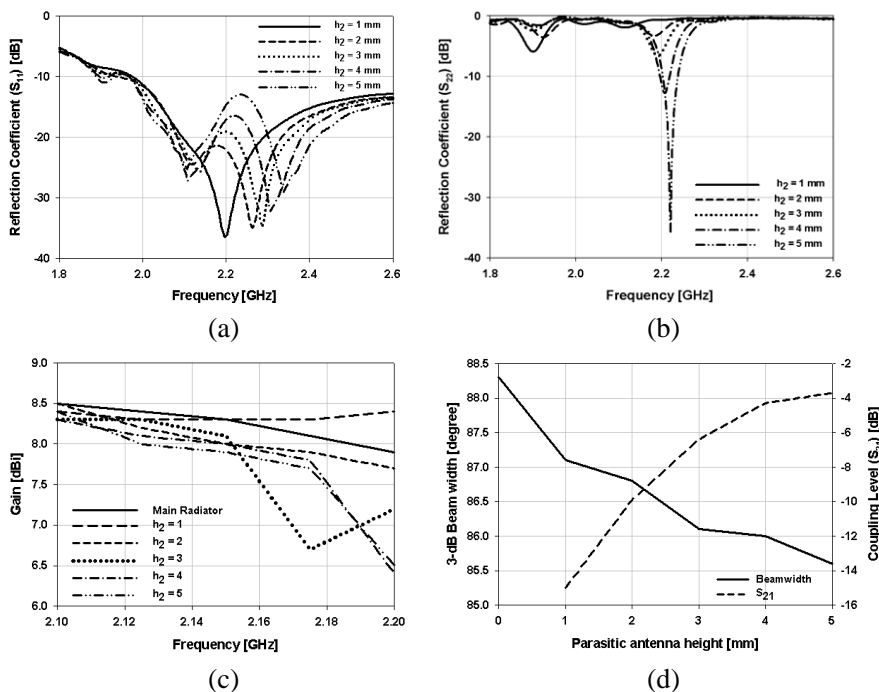
loop is 9 mm and the length ( $l_2$ ) is 57 mm. The overall lengths of the first and second turn of the parasitic radiator are nearly identical. As shown in Figure 1(b), the first turn of the parasitic radiator is excited by port 2 using a RF cable and its end is connected to the second loop via a through-hole in the substrate. The end of the second loop is connected to a ground pin which is connected to the antenna ground as well. The height of the parasitic loop can be controlled with a spacer, as shown in the upper diagram of Figure 1(a). The main radiator is placed in the center of the antenna ground and inserted into the rectangular slit of the substrate for the parasitic radiator. In this structure, the rectangular structure of the parasitic radiator minimizes the space occupied by the energy harvesting antenna, which is very favorable in the design of an array antenna.

Figure 3 shows the performance variation of the main radiator according to the height of the parasitic radiator in the simulation. As shown in Figure 3(b), the resonant frequency of the parasitic radiator increases from 2.15 to 2.20 GHz as the height increases and the return loss improves rapidly. However, although the resonance frequency of the main radiator is stable according to the height of the parasitic radiator, the return loss deteriorates. These results show that the influence of the parasitic radiator on the main radiator increases with the height of the parasitic radiator. In Figures 3(c) and (d), the coupling coefficient ( $S_{21}$ ) between the main and the parasitic radiator improves with the height of the parasitic radiator, but the gain and the 3-dB beamwidth of the main radiator decreases. The test results mentioned above are summarized in Table 1. From these results, we chose 2 mm as the optimal height of the parasitic radiator, as the gain of

**Table 1.** Performance variation of the main radiator according to the height of parasitic radiator (simulation).

Frequency [GHz]	2.100		2.150		2.200		$S_{21}$
	Gain	BW	Gain	BW	Gain	BW	
<b>Main radiator only</b>	<b>8.5</b>	<b>85.8</b>	<b>8.3</b>	<b>88.3</b>	<b>7.9</b>	<b>92.9</b>	-
$h_2 = 1$ mm	8.4	85.7	8.3	87.1	8.4	88.1	-15.0
$h_2 = 2$ mm	8.5	85.3	8.1	86.8	7.7	88.7	-10.1
$h_2 = 3$ mm	8.3	83.0	8.1	86.1	7.2	92.4	-6.4
$h_2 = 4$ mm	8.3	84.9	8.0	86.0	6.4	87.2	-4.3
$h_2 = 5$ mm	8.4	84.7	7.9	85.6	6.5	85.3	-3.7

\* Unit: Gain [dB],  $S_{21}$  [dB], BW (Beam width) [°]



**Figure 3.** Performance variation of the main radiator according to the height of the parasitic radiator. (a) Return loss of the main radiator. (b) Return loss of the parasitic radiator. (c) Gain performance of the main radiator. (d) 3-dB beam width and coupling level between the main and parasitic radiators at 2.15 GHz.

the main radiator is nearly identical to that of the model with only the main radiator (to within 0.2 dB), whereas the coupling characteristic,  $-10.1$  dB, is relatively high. The antenna simulation was done using the commercial simulation tool *CST Microwave Studio*®.

### 3. FABRICATION AND PERFORMANCE TEST

Figure 4 shows photos of the fabricated energy harvesting antenna. The antenna is composed of two main parts, the main radiator and the parasitic radiator. As shown in the figure, the main radiator is vertically placed in the center of the ground and is inserted into the rectangular slit of the parasitic radiator. As shown in Figure 4(b), the main radiator has a port named Port1, and the parasitic radiator is fed by Port2 into one end of the loop. The other end of the loop is

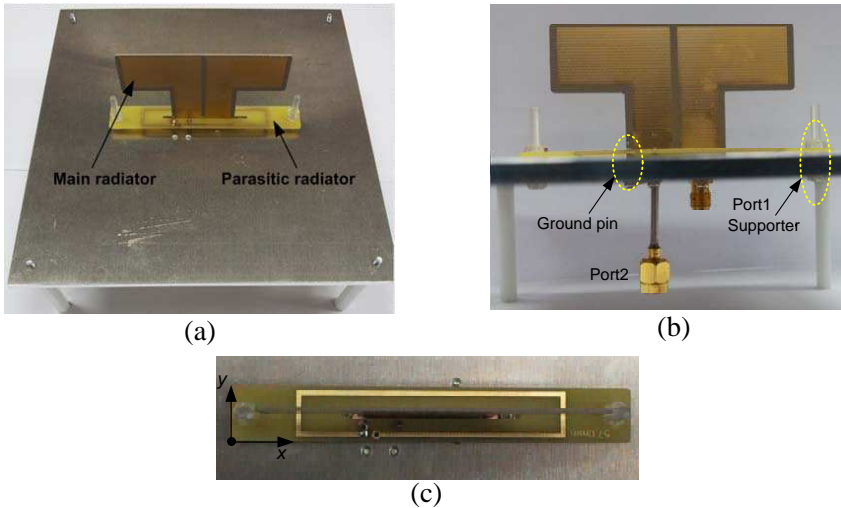


**Figure 4.** Fabricated proposed energy harvesting antenna. (a) Perspective view. (b) Side-view. (c) Top view.

connected to a metal ground plate using a ground pin. The ground size is  $100\text{ mm} \times 100\text{ mm}$ . Plastic supporters are placed at both ends of the substrate of the parasitic radiator to control the height. The fabricated antenna structure can be clearly understood from the top view of the fabricated antenna shown in Figure 4(c).

To verify the performance of the proposed antenna, we measured the antenna performance. The measured reflection coefficient of the main and the parasitic radiator according to the height of the parasitic radiator is presented in Figure 5. As shown in Figure 5(a), the reflection coefficient of the main radiator is degraded as the height of the parasitic radiator increases from 2 mm to 5 mm, but it is below  $-10\text{ dB}$  at all heights in the operating frequency range of 2.13 to 2.17 GHz. The performance of the parasitic radiator is increases as the height increases. Figure 5(b) shows that the parasitic radiator has a more distinct resonant characteristic at 2.18 GHz as the radiator's height increases. Although the reflection coefficient of the parasitic radiator is the worst above  $-5\text{ dB}$  when  $h_2 = 2\text{ mm}$ , the main radiator shows good performance below  $-15\text{ dB}$ . In this measured result, there is the large difference compared with the simulation result in Figure 3(b) which was considered to be caused by fabrication error for the parasitic radiator with a ground pin and a cable feeding.

Figure 6(a) shows the measured coupling coefficient ( $S_{21}$ ) between the main and the parasitic radiator. The coupling coefficient improves

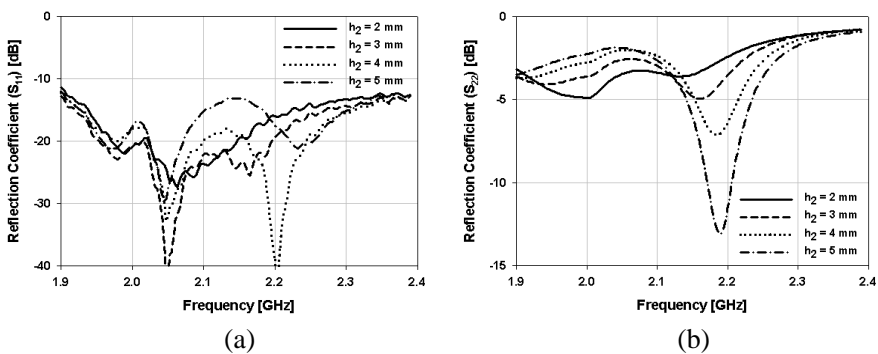


**Figure 5.** Measured reflection coefficient characteristic according to the height of parasitic radiator. (a) Main radiator. (b) Parasitic radiator.

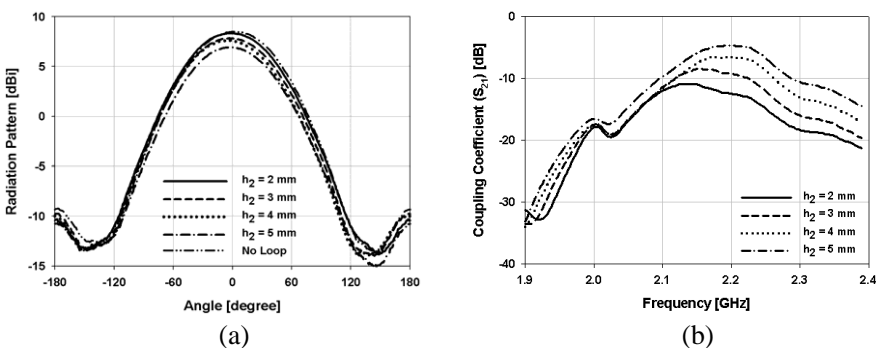


**Figure 6.** Measured proposed antenna performance according to the height of the parasitic radiator. (a) Coupling coefficient between the main and parasitic radiator. (b) Radiation pattern of main radiator on the  $E$ -plane.

as the height of the parasitic radiator increases, and the coupling coefficient is about  $-12$  dB when  $h_2 = 2$  mm. In contrast, the antenna gain of the main radiator gradually decreases. The main radiator without the parasitic radiator has a gain of 8.50 dBi, and the gain of the main radiator with the parasitic radiator ranges from 6.93 dBi to 8.35 dBi. The maximum gain of the fabricated antenna occurs when  $h_2 = 2$  mm. The 3-dB beamwidth of the main radiator when  $h_2 = 2$  mm is 87.1, which is slightly narrower than the beamwidth of the main radiator without the parasitic part, at 88.6. The radiation

pattern on the  $E$ -plane (the  $x$ -axis in the coordinate of Figure 4(c)) and the gain of the main radiator are presented in Figure 6(d). All patterns are measured in a far-field anechoic chamber with an antenna measurement system from Orbit Inc. The measurement frequency is 2.15 GHz, which is the center frequency of the operating bandwidth.

In addition to the electrical performance test of the fabricated antenna, we performed an EIRP (effective isotropically radiated power) test to verify the normal operation of the main radiator. As shown in Figure 7, a signal generator and a spectrum analyzer are placed separately 5 m apart. First, two standard gain horns having a gain of 10 dBi were used as the radiators for the instruments. The output power of the signal generator was 10 dBm at 2.15 GHz (a single tone of a continuous wave) and the RF cable loss was 0.75 dB. The calculated EIRP of the TX part was 19.25 dBm and the receiving power in the spectrum analyzer was  $-35.7$  dBm. Thus the measured free space loss was 54.2 dB. For the next step, the horn connected to the signal generator was exchanged with the main radiator without the parasitic radiator. In this test, the test setup is identical to the former test using two horns, while the receiving power is  $-37.45$  dB. In this case, the receiving power is lower than the first test by  $-0.2$  dB considering the difference in the antenna gain, at 1.5 dB. Finally, the fabricated energy harvesting antenna was used as the radiator of a signal generator. The receiving power was  $-37.95$  dBm, which is 0.6 dB lower than the receiving power of the first test. The coupled RF power was about  $-2.0$  dBm, which is a considerable amount of power compared to the harvested power of a conventional receiver, at  $-40$  to  $-20$  dBm. From these test results, it is verified that with the proposed antenna, we can harvest much RF energy to be converted to DC power for the operation of electronic devices without degrading the performance of the main radiator. All of test results are summarized in Table 2.

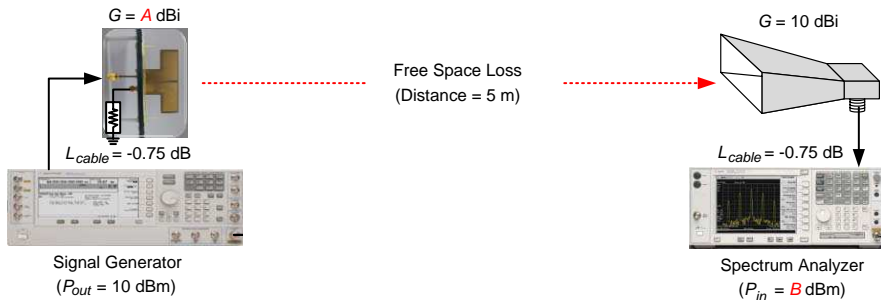


**Figure 7.** EIRP test setup using the fabricated energy harvesting antenna.

**Table 2.** Summary of EIRP test using several antennas.

TX antenna	TX antenna gain (A) [dBi]	EIRP [dBm]	FSL [dB]	Receiving power (B) [dBm]	Receiving power error for horn [dB]
Standard horn antenna	10.0	19.25	54.2	-35.70	-
Main radiator only	8.5	17.70		-37.45	-0.2
Proposed energy harvesting antenna	8.35	17.60		-37.95	-0.6

#### 4. CONCLUSION

At present, as new mobile services are introduced, interest in RF energy harvesting technology is increasing. To obtain high levels of RF energy from free space, many studies have focused on wide-band or multi-band structures with highly efficient rectifier modules. However, the harvested RF energy is too low to power electronic devices.

In this paper, a novel RF energy harvesting antenna is introduced. This antenna is designed to gather RF energy using a parasitic radiator from the main radiator of a variety of wireless transmitters (or transceivers) as used in the Korean WCDMA service. The main radiator is a printed dipole having several merits, including wideband operation and considerable gain. The parasitic radiator has a two-turn loop structure fabricated on a substrate. The parasitic radiator surrounding the main radiator receives the RF power radiated from the main radiator, which does not contribute to the main radiator's electrical performance. Thus, we can generate DC power using dissipated RF energy without a performance degradation of the main radiator.

The fabricated main radiator without the parasitic radiator has a gain of 8.50 dBi at 2.15 GHz. In the other hand, the main radiator with the parasitic radiator has a gain of 8.35 dBi when the height of the parasitic radiator is 2 mm. However, the parasitic radiator can

obtain a considerable amount of power from the main radiator due to the realized coupling performance of  $-12$  dB between the main and the parasitic radiator. Moreover, an EIRP test was conducted to confirm the performance of the antenna, showing that it is possible to harvest RF power of  $-2.0$  dBm when the antenna input power is  $9.25$  dBm. The output power of the signal generator is  $10$  dBm and the RF cable loss is  $0.75$  dB.

We anticipate that the proposed antenna can be used as an auxiliary DC power means in various wireless communication transceivers. In the future, we will devise a method to enhance the energy harvesting capacity of the proposed antenna.

## ACKNOWLEDGMENT

The authors would like to express their gratitude to Dr. I. G. Cho and Mr. S. M. Kim of ETRI for their valuable advice and contributions to the antenna design and related experiments.

This research was funded by the MSIP (Ministry of Science, ICT & Future Planning), Korea in the ICT R&D Program 2013, Development of RF Energy Transmission under 100 Watts and Harvesting Technology.

## REFERENCES

1. Paradiso, J. A. and T. Starner, "Energy scavenging for mobile and wireless electronics," *IEEE Pervasive Computing*, Vol. 1, No. 4, 18–24, 2005.
2. Bouchouicha, D., M. Latrach, F. Dupont, and L. Ventura, "An experimental evaluation of surrounding RF energy harvesting devices," *European Microwave Conference (EuMC)*, 1381–1384, Sep. 2010.
3. Georgiadis, A., G. Andia, and A. Collado, "Rectenna design and optimization using reciprocity theory and harmonic balance analysis for electromagnetic (EM) energy harvesting," *IEEE Antennas and Wireless Propagation Letters*, Vol. 9, 444–446, 2010.
4. Kim, P., G. Chaudhary, and Y. Jeong, "A dual-band RF energy harvesting using frequency limited dual-band impedance matching," *Progress In Electromagnetics Research*, Vol. 141, 443–461, 2013.
5. Md. Din, N., C. K. Chakrabarty, A. Bin Ismail, K. K. A. Devi, and W.-Y. Chen, "Design of RF energy harvesting system

- for energizing low power devices,” *Progress In Electromagnetics Research*, Vol. 132, 49–69, 2012.
6. Sim, Z. W., R. Shuttleworth, M. J. Alexander, and B. D. Grieve, “Compact patch antenna design for outdoor RF energy harvesting in wireless sensor networks,” *Progress In Electromagnetics Research*, Vol. 105, 273–294, 2010.
  7. Buonanno, A., M. D’Urso, and D. Pavone, “An ultra-wideband system for RF Energy harvesting,” *European Conference on Antennas and Propagation (EUCAP)*, 388–389, Apr. 2011.
  8. Ren, Y.-J. and K. Chang, “5.8-GHz circularly polarized dual-diode rectenna and rectenna array for microwave power transmission,” *IEEE Transactions on Microwave Theory and Techniques*, Vol. 54, No. 4, 1495–1502, 2006.
  9. Mikeka, C. H. Arai, A. Georgiadis, and A. Collado, “DTV band micropower RF energy-harvesting circuit architecture and performance analysis,” *IEEE International Conference on RFID-Technologies and Applications (RFID-TA)*, 561–567, Sep. 2011.
  10. Mikeka, C. and H. Arai, “Microwave tooth for sensor power supply in battery-free applications,” *Asia-Pacific Microwave Conference Proceedings (APMC)*, 1802–1805, Dec. 2011.
  11. Mikeka, C. and H. Arai, “Dual-band RF energy-harvesting circuit for range enhancement in passive tags,” *European Conference on Antennas and Propagation (EuCAP)*, 1210–1214, Apr. 2011.
  12. Heo, S., Y. S. Yang, J. Lee, S.-K. Lee, and J. Kim, “Efficient maximum power tracking of energy harvesting using a  $\mu$  controller for power savings,” *ETRI Journal*, Vol. 33, No. 6, 973–976, Dec. 2011.
  13. Shigeta, R., T. Sasaki, D. M. Quan, Y. Kawahara, R. J. Vyas, M. M. Tentzeris, and T. Asami, “Ambient RF energy harvesting sensor device with capacitor-leakage-aware duty cycle control,” *IEEE Sensors Journal*, Vol. 13, No. 8, 2973–2983, Aug. 2013.
  14. Rudge, A. W., K. Milne, A. D. Olver, and P. Knight, *Handbook of Antenna Design*, 2nd Edition, IEE Electromagnetic Wave Series, 1986.
  15. Sumner, D., *ON4UN’s Low-band DXing*, 4th Edition, No. 74 of the Radio Amateur’s Library, ARRL, 2005.